HHS Public Access

Author manuscript

Bioorg Med Chem. Author manuscript; available in PMC 2022 June 15.

Published in final edited form as:

Bioorg Med Chem. 2021 June 15; 40: 116183. doi:10.1016/j.bmc.2021.116183.

Spectroscopic and Biochemical Characterization of Metallo-β-lactamase IMP-1 with Dicarboxylic, Sulfonyl, and Thiol Inhibitors

Huan Zhang[a], **Kundi Yang**[a], **Zishuo Cheng**[a], **Caitlyn Thomas**[a], **Abbie Steinbrunner**[a], **Cecily Pryor**[a], **Maya Vulcan**[a], **Claire Kemp**[a], **Diego Orea**[a], **Chathura Paththamperuma**[a], **Allie Y. Chen**[b], **Seth M. Cohen**[b], **Richard C. Page**[a], **David L. Tierney**[a], **Michael W. Crowder**[a,*]

[a]Department of Chemistry and Biochemistry, Miami University, Oxford, OH 45056, USA

[b]Department of Chemistry and Biochemistry, University of California San Diego, La Jolla, CA 92093, USA

Abstract

In an effort to probe the biophysical mechanisms of inhibition for ten previously-reported inhibitors of metallo-β-lactamases (MBL) with MBL IMP-1, equilibrium dialysis, metal analyses coupled with atomic absorption spectroscopy (AAS), native state mass spectrometry (native MS), and ultraviolet-visible spectrophotometry (UV-VIS) were used. 6-(1*H*-tetrazol-5-yl) picolinic acid (1T5PA), ANT431, *D/L*-captopril, thiorphan, and tiopronin were shown to form IMP-1/Zn(II)/inhibitor ternary complexes, while dipicolinic acid (DPA) and 4-(3-aminophenyl)pyridine-2,6-dicarboxylic acid (3AP-DPA) stripped some metal from the active site of IMP but also formed ternary complexes. DPA and 3AP DPA stripped less metal from IMP-1 than from VIM-2 but stripped more metal from IMP-1 than from NDM-1. In contrast to a previous report, pterostilbene does not appear to bind to IMP-1 under our conditions. These results, along with previous studies, demonstrate similar mechanisms of inhibition toward different MBLs for different MBL inhibitors.

Graphical Abstract

*Address correspondence to Michael W. Crowder, 651 E. High St, 160 Hughes Laboratories, Oxford, OH 45056, USA crowdemw@miamioh.edu.

Declaration of interests

The authors declare that they have no known competing financial interests or personal relationships that could have appeared to influence the work reported in this paper.

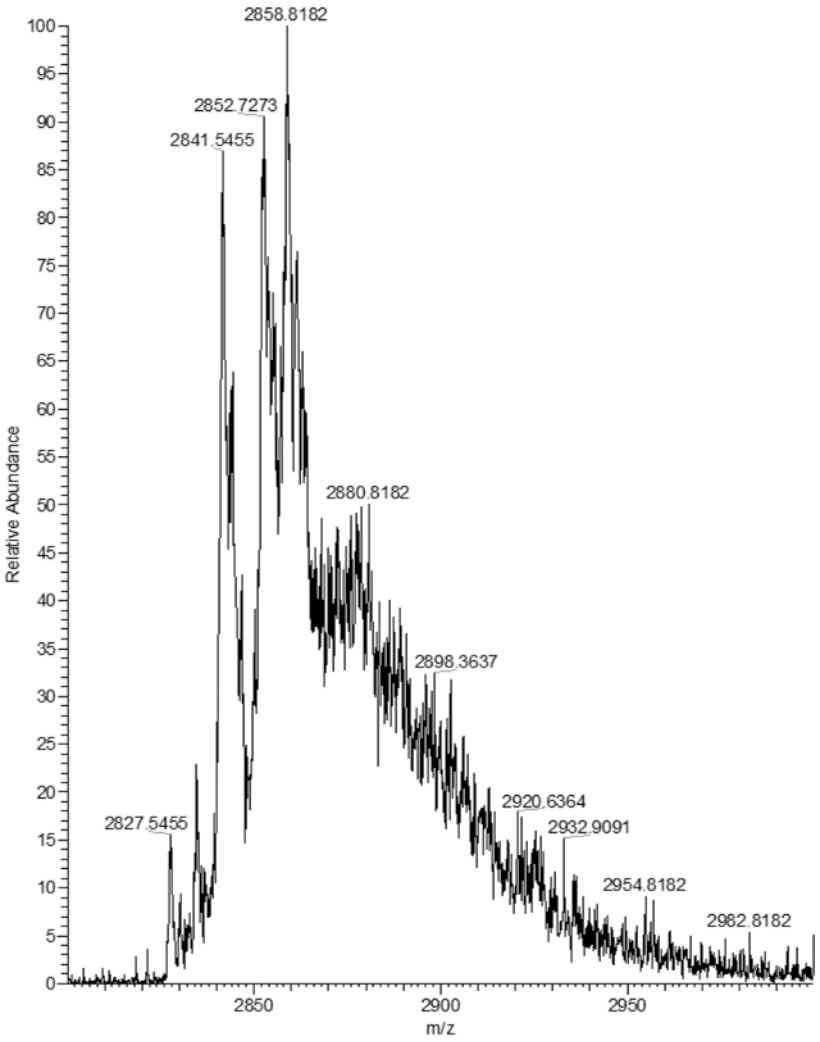

Keywords

Antibiotic resistance; metallo-β-lactamase; IMP-1; MBL inhibitors; native state mass spectrometry

1. Introduction

The production of β-lactamases is a primary cause for clinical resistance to β-lactam antibiotics in Gram-negative bacteria, such as penicillins, cephamycins, carbapenems, and cephalosporins, that are used to combat bacterial infections.[1] Antibiotic resistance is a global threat with annual deaths totaling >23,000 in the U.S., >25,000 in the European Union, >58,000 infant deaths in India, and >38,000 deaths in Thailand, according to a Centers of Disease Control report in 2019.[2] The 4,953 identified β-lactamases can be grouped into four different classes: A, B, C, and D based on amino acid sequences and molecular characteristics.[3] Class A, C, and D β-lactamases hydrolyze the β-lactam ring in most β-lactam containing antibiotics, using an active site serine residue, and there are clinically-available inhibitors like clavulanate that are active against some of these β-lactamases.[4]

Class B β-lactamases are also called metallo-β-lactamases (MBLs) because they utilize 1-2 Zn(II) ions to hydrolyze the β-lactam ring, and currently, there are no clinically-available inhibitors to treat infections caused by bacteria that harbor an MBL.[5] Therefore, there have been considerable efforts to discover inhibitors for many years, and to date, there are several classes of *in vitro* MBL inhibitors. These include metal-ion binding inhibitors, covalent inhibitors, allosteric inhibitors, and a host of inhibitors with uncharacterized mechanisms.[6]

Class B β-lactamases can be further divided into three subgroups (B1, B2, and B3) based on their metal-binding and catalytic properties. However, different MBLs from different subclasses, and even members of the same subclass, display functional differences, due to low sequence similarities.[7] Subclass B1 contains the largest number of β-lactamases, and many of these enzymes have large numbers of characterized clinical variants. Also the corresponding bacterial carriers are disseminating all over the world with NDMs (New Delhi Metallo-β-lactamase) dominantly spreading in India and Pakistan, VIMs (Verona Integron-encoded Metallo-β-lactamases) mainly circulating in Russia, China, and Canada, and IMPs (IMiPenemases) primarily distributing in Japan, Argentina, and Thailand.[8] Previous studies have shown that NDM and VIM are evolving because of the scarcity of Zn(II) *in vitro*, and mechanism of inhibition studies on NDM and VIM with many MBL inhibitors have been reported.[9, 10, 11, 12] While some inhibitors of IMP-1 have been reported,[3,16] there have been relatively few reports showing the mechanism of inhibition for any MBL inhibitors with IMP-1. More importantly, NDMs, VIMs, and IMP-1 exhibit very distinct K_M, k_{cat}, and IC_{50} values with the same substrates and inhibitors.[13] Therefore, there is still an urgent need to probe the mechanism of inhibition for IMP with current available inhibitors.

The bla_{IMP} gene that encodes IMP was initially found in clinical, imipenem-resistant *Serratia marcescens* and *Pseudomonas aeruginosa* isolates in Japan, and IMP was the first identified transferable MBL.[14, 15] The IMP enzymes belong to the B1 subclass and exhibit broad substrate specificities, and 85 variants have been found to date.[3] IMP variants exhibit higher affinities for cephalosporins and carbapenems over penicillins. IMP-1, the first variant identified, is the most studied IMP variant, and there have been many inhibitors of IMP-1 reported.[3,16] While there have been many crystal structures of MBL-inhibitor complexes, many other inhibitor studies, especially those that do not have crystal structures, only report IC_{50} and/or MIC (minimum inhibitory concentration) values, and most of the reported inhibitors have not been characterized for mechanism of inhibition.[6] This lack of understanding negatively impacts efforts within the research community to find clinically-relevant inhibitors of the IMP variants, and other MBLs.

In this study, we probed the mechanism of inhibition of 10 previously-reported MBL inhibitors with IMP-1 (Table 1). We report here spectroscopic and biochemical studies, including equilibrium dialysis, coupled with metal analyses, and native state mass spectrometry, to probe whether these inhibitors strip Zn(II) from IMP-1 or enzyme-metal-inhibitor ternary complexes are formed. Ultraviolet–visible spectrophotometry (UV-vis) with Co(II)-substituted analogs of IMP-1 were used to probe whether ternary complex-forming inhibitors bind to one or both of the metal ions. The data presented demonstrate that 1T5PA, ANT431, captopril, thiorphan, and tiopronin form ternary complexes with IMP-1, while EDTA, 3AP-DPA, and DPA appear to strip metal from IMP-1 under the conditions

employed. In contrast to a previous report,[24] pterostilbene exhibited no binding to IMP-1 or to IMP variants, and we cannot determine the mechanism of inhibtion for 2,3-demercaprol. We also examined whether the IMP-6 (S262G), IMP-10 (V67F), and IMP-78 (S262G/V67F) variants form ternary-complexes with 1T5PA, ANT431, captopril, thiorphan, and tiopronin.

2. Materials and Methods

2.1 Materials.

IMP plasmids for over-expression were obtained as described below. The pET-28a (+)-TEV-IMP-1 over-expression plasmid was prepared by synthesizing and inserting the IMP-1 DNA sequence from residues 19 to 246, which was codon-optimized for *E. coli*, into a pUC57 vector, followed by subcloning the IMP-1 gene into pET-28a (+)-TEV (using the restriction sites *Nde*I and *Xho*I). The over-expression plasmids for the S214G and V49F variants of IMP (IMP-6 and IMP-10, respectively) were generated by side-directed mutagenesis. The IMP-78 over-expression plasmid was obtained using the pET-28a (+)-TEV-IMP-10 plasmid as the template and site-directed mutagenesis. Isopropyl β-*D*-thiogalactoside (IPTG) was purchased from Gold Biotechnology (St. Louis, MO). Miller Luria-Bertani (LB) growth medium, dialysis tubing, Slide-A-Lyzer Cassettes, EDTA, and all of the buffers were purchased from ThermoFisher Scientific (Waltham, MA). HisTrap™ HP columns and the ÄKTA™ start protein purification system were procured from GE Healthcare (Chicago, IL). Dithioglycerol, pterostilbene, and thiorphan were purchased from Sigma-Aldrich (St. Louis, MO). *L*-Captopril and tiopronin were obtained from Acros Organics (Fair Lawn, NJ), ANT-431 was a gift from Dr. Marc Lemonnier.[12] 4-(3-Aminophenyl) pyridine-2,6-dicarboxylic acid (3AP-DPA), 6-(1H-tetrazol-5-yl) picolinic acid (1T5PA), and DPA were provided by the laboratory of Professor Seth Cohen at the University of California at San Diego. Bio-Rad Chelex-100 resin was used (Hercules, CA) to remove metals for all of the buffer solutions prepared for UV-VIS. Bio-Rad Micro Bio-Spin™ 6 columns were purchased to desalt IMP samples for native mass spectrometry.

2.2 Over-expression and purification of IMP-1 and IMP variants.

The over-expression plasmids of IMP-1, IMP-6, IMP-10, and IMP-78 were transformed into BL21(DE3) *E. coli* cells, and the resulting colonies were plated on LB-agar plates containing 50 μg/mL kanamycin. A single colony was used to inoculate a 50 mL LB starter culture containing 50 μg/mL kanamycin, and the culture was shaken overnight at 37 °C. A 10 mL portion of the starter culture was transferred to 6 × 1L LB cell culture flasks containing 50 μg/mL kanamycin. These flasks were shaken at 37 °C until the cultures reached an $OD_{600\ nm}$ (Optical Density at 600 nm) of 0.6 to 0.8. The culture flasks were cooled at room temperature, and then each flask was made 10 μM in $ZnCl_2$ and 0.5 mM in IPTG. The flasks were shaken at 18 °C overnight. The cells were harvested by centrifugation at 7,500 rpm for 15 minutes. The collected cells were resuspended with 50 mM HEPES (4-(2-hydroxyethyl)-1-piperazineethanesulfonic acid), pH 7.5, containing 500 mM NaCl, and the resuspended cells were ruptured by passing them through a French Press three times at 15,000 psi (cell pressure). Benzonase nuclease (100 μg; Millipore Sigma, Burlington, MA) was added to the ruptured cell mixture, which was then centrifuged at 15,000 rpm. The clarified supernatant was loaded onto the HisTrap™ HP column, and the column was

washed with 40 mL of 50 mM HEPES, pH 7.5, containing 500 mM NaCl. His-tagged IMP was eluted from the column by using 50 mM HEPES, pH 7.5, containing 500 mM NaCl and 500 mM imidazole. The eluted protein was incubated with TEV (Tobacco Etch Virus) protease at a ratio of His_6-IMP-1: TEV of 50:1 (v: v) for 10 minutes. The mixture was dialyzed versus 50 mM HEPES, pH 7.5, containing 500 mM NaCl for 4 hours to remove the imidazole. The resulting mixture was loaded onto the HisTrap™ HP column, and IMP-1 (and IMP variants) was collected.

2.3 Characterization of purified IMP-1 and IMP variants.

The concentrations of purified IMP-1 and IMP variants were determined using UV-VIS absorbance at 280 nm with corresponding extinction coefficients, calculated by using ExPASy ProtParam (ε_{280nm} = 46,410 M^{-1} cm^{-1} for His_6-IMP-1 and variants and ε_{280nm} = 44,920 M^{-1} cm^{-1} for IMP-1 and variants).[25] Purified His_6-IMP-1, IMP-1, and IMP variants were analyzed for purity by using sodium dodecyl sulfate-polyacrylamide gel electrophoresis (SDS- PAGE). The zinc content of the IMP samples was determined by using a PerkinElmer PinAAcle 500 Atomic Absorption Spectrometer (AAS), as previously described.[17, 22] $ZnCl_2$ (to reach 2 molar equivalents) was added to any samples that had less than 2 equivalents of Zn(II), and the resulting mixtures were dialyzed against 2L of 50 mM HEPES, pH 7.5, containing 500 mM NaCl overnight at 4 °C. The final zinc content was determined by using AAS.

2.4 Steady state kinetics of IMP-1 with meropenem.

IMP stock solutions (4 μM) and 10 mM meropenem were prepared in 50 mM HEPES, pH 7.5, containing 150 mM NaCl and 50 μM $ZnCl_2$. The hydrolysis of meropenem was followed at 298 nm (ε_{298nm} = 7,200 $M^{-1}cm^{-1}$) on a Hewlett-Packard 5480A UV-VIS (Agilent, Santa Clara, CA) spectrophotometer at 25 °C.[26] The values of K_M and k_{cat} were determined by fitting the data to the Michaelis-Menten equation using Prism GraphPad (2018 GraphPad Software).

2.5 Equilibrium dialyses and metal analyses.

Before equilibrium dialyses, IMP samples were dialyzed against 2L of 50 mM HEPES, pH 7.5, at 4 °C to remove any loosely-bound Zn(II). Sample (5 mL) of 8 μM IMP were incubated on ice with 0, 2, 4, 8, and 16 molar equivalents of inhibitor for an hour, and the samples were then dialyzed versus 50 mM HEPES, pH 7.5, at 4 °C for 4 hours. The metal content of the IMP samples was determined by AAS.[17, 22]

2.6 Native mass spectrometry of IMP/inhibitor complexes.

Before mass spectrometry, 50 μM samples of IMP were desalted by passing the solution through Micro Bio-Spin™ 6 columns three times. The desalted IMP samples were diluted to 10 μM and incubated with 5 molar equivalents of each inhibitor on ice for at least 10 minutes. Next, positive mode protein detection was used with the nano-electrospray ionization (n-ESI) probe (Thermo Fisher Scientific, San Jose, CA, USA) on a Thermo Scientific LTQ Orbitrap XLTM hybrid ion trap-orbitrap mass spectrometer. The parameters for collecting the spectra were described previously.[9]

2.7 UV-VIS spectra of IMP with inhibitors.

In order to obtain metal-free IMP-1, 300 μM IMP-1 was initially dialyzed two times versus 500 mL of 50 mM HEPES, pH 6.8, containing 500 mM NaCl, 2 mM EDTA, and 0.5 grams of Chelex-100 at 4 °C and then 3 times against 500 mL of 50 mM HEPES, pH 6.8, containing 500 mM NaCl and 0.5 grams of Chelex-100 at 4 °C. Each dialysis step was 8-10 hours. The resulting metal-free IMP-1 sample was concentrated to ~0.5 mM. IMP-1 was diluted with 50 mM HEPES, pH 6.8, containing 500 mM NaCl, 10% glycerol and 2 mM TCEP (*tris*(2-carboxyethyl) phosphine), and then 2 molar equivalents of Co(II) were added, followed by incubating on ice for 5 minutes to ensure uptake by the enzyme. Inhibitors were then added, and the mixture was incubated on ice for another 5 minutes. A PerkinElmer Lambda 750 UV/vis/NIR spectrometer was used to collect spectra between 250 and 800 nm at room temperature, and the signal was recorded as absorbance. The UV-vis spectrum of metal-free IMP-1 was used to generate the difference spectra shown.

3. Results

3.1 Over-expression, purification, and characterization of IMP-1 and IMP variants.

IMP-1 and IMP variants were over-expressed and purified. SDS-PAGE gels revealed that the isolated enzyme samples were >95% pure. Metal analyses showed that newly-purified IMP-1 binds 1.2 ± 0.2 equivalents of Zn(II); however, the addition of $ZnCl_2$ followed by dialysis resulted in IMP samples containing 2.0 ± 0.1 equivalents of Zn(II) (see Materials and Methods for details). Steady-state kinetics with meropenem as the substrate yielded k_{cat} and K_M values of 7 ± 1 s^{-1} and 9 ± 2 μM, respectively, which are slightly different (less than a factor of 3 for k_{cat}) than those previously-reported possibly due to different over-expression constructs and buffer systems (26 s for k_{cat} and 6.5 μM K_M in 50 mM phosphate buffer, pH 7.0, containing 50 μM $ZnCl_2$ at 25 °C).[26] The predicted molecular weights for IMP-1, IMP-6, IMP-10, and IMP-78 are 25,438.09 Da, 25,456.11 Da, 25,408.07 Da, and 25,486.14 Da, respectively, and native mass spectra of the IMP-1 and IMP variants revealed masses of 25,441.21 Da, 25,457.64 Da, 25,408.55 Da and 28,482.19 Da for IMP-1, IMP-6, IMP-10, and IMP-78, respectively (all within ± 0.01%).

3.2 Equilibrium dialyses and metal analyses.

In an effort to determine the mechanism of inhibition for the inhibitors with IMP-1, we conducted equilibrium dialyses and analyzed the dialyzed samples for metal content, as previously described.[17] After purification, we exhaustively dialyzed IMP-1 to remove any loosely-bound Zn(II). Similar to previously-published data for NDM-1, VIM-2, and IMP-7,[27] the resulting enzyme samples bound slightly less than 2 equivalents of Zn(II) (for 10 separate samples, IMP-1 bound 1.7 ± 0.1 equivalents of Zn(II)). As previously reported,[19,23] we utilized EDTA as a metal stripping agent and captopril, which has been shown to form ternary complexes with other MBLs, as controls. For IMP-1, EDTA removed nearly 1.0 equivalent of Zn(II) (Figure 1, blue dots), while captopril did not remove Zn(II) from the enzyme (Figure 1, orange diamonds). 3AP-DPA appeared to strip Zn(II) from IMP-1 but at not the same extent as EDTA (Figure 1, purple diamonds). The remaining compounds, DPA, 2,3-dimercaprol, ANT431, thiorphan, tiopronin, pterostilbene, and 1T5PA, did not appear to remove appreciable amounts of Zn(II) under the conditions used in this experiment,

removing less that 0.3 equivalents of Zn(II).[17, 18, 19, 20, 22, 24] This result was surprising for DPA, which is a known metal stripping agent for other MBLs, and 2,3-dimercaprol, which was recently shown to strip metal from VIM-2.[9]

3.3 Native mass spectrometry of IMP-1/inhibitor complexes.

In order to probe further whether ternary complexes were formed between IMP-1, Zn(II), and the inhibitors, we utilized native mass spectrometry, as previously described.[9, 28] Initially, IMP-1 alone was investigated, and the native MS spectrum showed that the dominant peaks are at 2,557.9979 m/z, 2,842.3565 m/z, and 3,197.0346 m/z, which correspond to the masses of +10, +9, and +8 IMP-1 with two equivalents of Zn(II), respectively (Figure 2 and Table S1). No peaks corresponding to apo-IMP-1, or IMP-1 with one equivalent of bound Zn(II) were observed, indicating that the binary enzyme:2Zn complexes could be analyzed using native MS. Since the +9 peak is often the most intense under the conditions that we used to obtain the native MS, we will focus on these peaks when describing spectra of the enzyme containing the inhibitors below.

The dicarboxylic derivatives, DPA, 1T5PA, and 3AP-DPA, were studied by incubating 10 μM IMP-1 with 5 equivalents of inhibitors on ice for 5 minutes. The native MS spectrum of IMP-1 containing DPA showed a dominant peak corresponding to ZnZn-IMP-1 plus 1 equivalent of DPA; however, there are peaks in the spectrum that correspond to Zn-IMP-1 plus 1 equivalent of DPA, apo IMP-1, and ZnZn-IMP-1 with no bound DPA (Figure 3A and Table S2). In contrast to a recent report with VIM-2,[9] we did not observe a peak corresponding to metal-free IMP-1 bound to 1 equivalent of DPA. For spectra with 1T5PA, the dominant peak corresponds to ZnZn-IMP-1 with no bound 1T5PA, but there is a visible peak, corresponding to ZnZn-IMP-1 bound to 1 equivalent of 1T5PA (Figure 3B and Table S2), indicating weak ternary complex formation. In the native MS with 3AP-DPA and IMP-1, the dominant peak corresponds to ZnZn-IMP-1 with no 3AP-DPA bound, however, the spectrum also shows Zn-IMP-1 plus 1 equivalent 3AP-DPA and ZnZn-IMP-1 plus one equivalent 3AP-DPA, again indicating weak complex formation; there was no evidence of a peak corresponding to metal-free IMP-1 (Figure 3C and Table S2).

The sulfonyl compound ANT431, which has been recently shown to form ternary complexes with VIM-2 and NDM-1,[9, 10] also forms a ternary complex with ZnZn-IMP-1, and the dominant peak corresponds to this complex. However, there is a peak that corresponds to unbound ZnZn-IMP-1 (*i.e.*, no ANT431 bound), and a small peak corresponding to Zn-IMP-1 bound to ANT431 (Figure 3D and Table S2).

We also probed the binding of the thiol compounds captopril, thiorphan, tiopronin and 2,3-dimercaprol, to IMP-1 using native MS. The dominant peak showed the presence of ZnZn-IMP-1 bound to captopril; however, there was a peak that corresponds to unbound ZnZn-IMP-1 (Figure 3E and Table S2). For thiorphan, the dominant peak corresponded to ZnZn-IMP-1 with thiorphan bound, and there are peaks corresponding to unbound ZnZn-IMP-1 and possibly Zn-IMP-1 with thiorphan bound (Figure 3F and Table S2). For tiopronin, the dominant peak corresponds to ZnZn-IMP-1 bound to tiopronin, and there is a significant peak corresponding to unbound ZnZn-IMP-1 (Figure 3G and Table S2). However, the native

MS spectrum of 2,3-dimercaprol with IMP-1 revealed a dominant peak corresponding to unbound ZnZn-IMP-1 (Table S2 and Figure S1), and no other peaks could be assigned.

The inhibition mechanism of EDTA with IMP-1, which was previously reported to be metal stripping for other MBLs,[9, 10] was also investigated. Interestingly, the dominant peak dominant native MS peak corresponds to ZnZn-IMP-1 with no bound inhibitor, but there is a small visible peak corresponding to metal-free IMP-1, without bound inhibitor (Figure S1 and Table S1). We speculate that our inability to observe a dominant peak corresponding to the metal-free IMP-1 may be due to metal-free IMP-1 binding adventitious Zn(II) before we loaded the sample into the mass spectrometer. This same event could have occurred with 2,3-dimercaprol. Therefore, we prepared metal-free IMP-1 and obtained the native MS (Figure S1). The spectrum showed the presence of peaks corresponding to metal-free IMP-1, Zn-IMP-1, and ZnZn-IMP-1 (Table S1). The dominant peak had a mass of 2,854.445 m/z, which may correspond to metal-free IMP-1 bound to 1 equivalent of buffer HEPES; although this assignment is tentative. Pterostilbene has also been studied here; however, the peak corresponding to ZnZn-IMP-1 with no bound inhibitor was the only peak observed (Figure S1).

Previous studies showed that different variants of IMP exhibit different steady-state kinetic constants and minimum inhibitory concentration (MIC) values with some of these inhibitors.[29, 30, 31, 32] Recently, we have studied IMP-6, IMP-10, and IMP-78 and posited that these variants are evolving due to overuse of carbapenems.[13] In that work, we showed that the mutations in IMP-6, IMP-10, and IMP-78, when compared to IMP-1, caused shifts in the positions of the metal ions and affected the position of Trp64 over the active site, which putatively lead to changes in the positions of substrates and in changes in catalysis.[13] We wanted to examine whether the mutations in the variants resulted in different interactions with the inhibitors tested herein. Therefore, we obtained the native MS of these variants with 1T5PA, ANT431, captopril, thiorphan, and tiopronin. For IMP-6, the native MS spectra with 1T5PA, ANT431, captopril, thiorphan, and tiopronin all showed dominant peaks that correspond to ZnZn-IMP-6 with no bound inhibitors. However, all the spectra have visible peaks for ZnZn-IMP-6 bound with 1 equivalent of inhibitor (Figure S2 and Table S4). For IMP-10 with 1T5PA, ANT431, and thiorphan, the native MS spectra also exhibited dominant peaks corresponding to ZnZn-IMP-10 with no bound inhibitors but exhibited visible peaks corresponding to the inhibitor-bound form. With captopril and tiopronin and IMP-10, the dominant peaks correspond to ZnZn-IMP-10 bound to 1 equivalent of inhibitor; however, there are visible peaks corresponding to ZnZn-IMP-10 with no bound inhibitors (Figure S3 and Table S4). For IMP-78 with 1T5PA, captopril, and thiorphan, the native MS spectra have dominant peaks corresponding to ZnZn-IMP-78 with no bound inhibitors; however, there are visible peaks corresponding to ZnZn-IMP-78 bound with 1 equivalent inhibitor. For IMP-78 with ANT431 and tiopronin, the native MS spectrum has a dominant peak corresponding to ZnZn-IMP-78 bound to 1 equivalent of inhibitor; however as with the other IMP variants, there are visible peaks corresponding to ZnZn-IMP-78 with no bound inhibitors (Figure S4 and Table S4).

3.4 Inhibitor binding to Co(II)-substituted IMP-1.

Results from native MS can only show whether inhibitors bind to ZnZn-IMP-1, but MS cannot demonstrate if the inhibitor coordinates directly to the active site metal ions or to which metal ion if the inhibitor only coordinates one of them. Therefore, Co(II)-substituted IMP-1 and UV-vis spectrophotometry were used to interrogate the IMP-1/inhibitor complexes.[33] The UV-vis spectrum of CoCo-IMP-1 exhibits an intense peak around 350 nm, which is attributed to a Cys-S to Co(II) ligand to metal charge-transfer (LMCT; ε_{350nm} ~ 1,500 $M^{-1}cm^{-1}$) that has been observed in other Co(II)-substituted MBLs including IMP-1 (Figure 4A).[34] In addition, as observed with other Co(II)-substituted MBLs, there are multiple broad peaks between 500 and 650 nm (ε_{550nm} ~ 200 $M^{-1}cm^{-1}$), which are attributed to high-spin Co(II) ligand field transitions (Figures 4A and 4B). [9, 10, 17, 22, 23]

The addition of 1 or 2 equivalents of EDTA resulted in a shift and a reduction of the LMCT band (ε_{350nm} ~ 900 $M^{-1}cm^{-1}$) and the loss of any features in the region between 500-650 nm (Figure 4C). This result is consistent with the equilibrium dialysis results, which showed the loss of only 1 metal ion, at > 10 eq of EDTA. The loss of features corresponding to the ligand field transitions, without loss of the CT band, suggests that Co(II) was removed from the consensus Zn1 site and that the remaining Co(II) is six-coordinate (expected ε_{550nm} < 30 $M^{-1}cm^{-1}$) (Figure S5E).[9, 10, 23] In contrast, the addition of captopril to CoCo-IMP-1 resulted in an increase in intensity and shift of the LMCT band, coupled with an increase in intensity and change in shape of the ligand field bands, in agreement with previous studies. [9, 10, 23] This result suggests a similar bridging binding mode for captopril when bound to CoCo-IMP-1.

However, the binding of dicarboxylic derivatives 1T5PA, DPA, and 3AP-DPA to Co(II)-substituted IMP-1 is different. The addition of 1T5PA, which was shown to bind to NDM-1,[17] resulted in UV-vis spectra with increased intensity of the LMCT (ε_{350nm} ~1,800 $M^{-1}cm^{-1}$) and decreased intensity of the d-d transitions (ε_{550nm} ~160 $M^{-1}cm^{-1}$) when 2 equivalents of 1T5PA were added (Figure 4E and 4F). Clearly, 1T5PA is binding to IMP-1, possibly at the Zn2 site (leading to the increase in extinction coefficient), but some of the metal ion, presumably at the Zn1 site, is removed at greater than 1 equivalent of inhibitor. The addition of DPA and 3AP-DPA resulted in similar spectra, suggesting the binding of both compounds to Co(II)-substituted IMP-1, although the addition of 1 equivalent of 3AP-DPA results in a reduction in the intensities of the d-d transitions, suggesting that more metal is removed from IMP-1 in the presence of this inhibitor (Figure S5 A, B, C and D).

The addition of ANT431, which was shown crystallographically to coordinate the Zn2 metal ion in VIM-2,[18] resulted in a large increase in the intensity of the LMCT (ε_{350nm} >2,500 $M^{-1}cm^{-1}$) and significant broadening of (and possible decrease in) the d-d transitions (Figure 5A and 5B), similar to the results for the dicarboxylates.[9, 18]

The thiol-based inhibitors have been shown to form ternary complexes with NDM-1 and showed increased LMCT intensities.[10] However in our study with IMP-1, there were only small changes in the intensities of the LMCTs (Figure 5C and 5E) after addition of tiopronin and thiorphan; the changes in the d-d transitions with IMP-1 were similar to those reported for NDM-1 (Figure 5D and 5F).[9] The UV-vis spectra after addition of 2,3-dimercaprol and

pterostilbene showed significant broadening of the LMCT bands (Figure S5F), which limited further investigation of these compounds. To ensure we were not observing complexes formed from the inhibitors and free Co(II), spectra of the inhibitors with Co(II) alone were also collected (Figure S6), indicating no significant complexation of free Co(II) in the enzyme spectra.

4. Discussion

Modern antibiotics, which were discovered 70-100 years ago,[35] have been used successfully to combat serious bacterial infections. However, many bacteria have acquired genes, which confer antibiotic resistant phenotypes, allowing many clinical strains to survive all known antibiotics.[36] Since β-lactam containing antibiotics are the largest class of antibiotics, β-lactamases are one of the main contributors to antibiotic resistance, and these enzymes are evolving continually under different selective pressures.[11, 12] Particularly, the class B β-lactamases (MBLs) have been a challenging target in the clinic for almost three decades, and to date, there are no clinically-available inhibitors towards them. Determining the mechanism of inhibition of new and existing MBL inhibitors is valuable for fully understanding current inhibitors and for focusing future inhibitor design efforts on compounds that form ternary complexes with the MBLs.[6, 9, 10, 11, 12, 17, 20, 22, 27] Since different MBLs exhibit different steady state kinetics values and different MIC results, we have also probed different MBLs (focusing on NDM-, VIM-, and IMP-)[9, 10, 27] and clinical variants of these MBL's.[11, 12] In this work, we report inhibition results on IMP-1 and several clinically-important IMP variants.

D/L-Captopril, thiorphan, tiopronin, and 2,3-dimercaprol are thiol-based inhibitors that are promising candidates as MBL inhibitors because Zn(II) is thiophilic, and captopril is already an FDA-approved drug, albeit for hypertension.[37] Previous work by Siemann *el al.* reported that thiol compounds (including tiopronin and 2,3-dimercaprol discussed in this present work) exhibit instantaneous or slow binding inhibition, depending on the charge state of the thiol compounds.[21] The authors speculated that one potential explanation of the time-dependent inhibition is isomerization of the enzyme-thiol complex with the thiol compound bound in a monodentate fashion to a μ-S bridged species; thiols with anionic substituents were proposed to isomerize quickly while thiols with neutral substituents isomerized slowly.[21] While this may occur for some thiol compounds and IMP-1, a recent crystal structure shows monodentate binding of tiopronin to NDM-1.[38]

Similar to results on other MBLs, UV-vis, equilibrium dialyses, and native MS show that captopril, thiorphan, and tiopronin clearly form ternary complexes with IMP-1, coordinating the metal centers similar as NDM-1 and VIM-2.[9, 10] Also like with VIM-2 and NDM-1, the dithiol, 2,3-dimercaprol, appears to strip metal from IMP-1. We cannot unambiguously determine the mechanism of inhibition with 2,3-dimercaprol but our results are identical to those reported by Siemann *et al.* who used ESI-MS to probe the metalation of IMP-1.[21] In that work, the authors reported that only the ZnZn analog of IMP-1 was detected after removal of the dithiol compound.[21] In fact, Siemann *et al.* initially reported the use of ESI-MS to probe the metalation state of IMP-1 after incubation with metal chelators.[39] In both studies, the authors assumed that the volatilization and ionization of all IMP-1 species were

identical so that peak areas were directly correlated to the concentration of the species in the liquid sample.[21, 39] This present work and previous native MS studies from our group demonstrate that this assumption is most likely not correct.[9, 10] In addition, the authors of these previous studies apparently did not consider whether metal-free analogs of IMP-1 could bind adventitious Zn(II) during before or during ESI-MS data acquisition. Our current studies also strongly suggest that this possibility is real and must be considered when interpreting ESI/native MS data on metalloenzymes.[9, 10]

With the IMP variants, native mass spectra suggest a possible difference in binding between the variants and captopril, tiopronin, and thiorphan. The dominant peaks with IMP-6 correspond to ZnZn-IMP-6 with no inhibitor bound, while for IMP-1, the dominant peak corresponded to the ternary complex for each case. For IMP-10 and IMP-78, the dominant peaks for the thiorphan samples correspond to the unbound ZnZn-IMP-10 or ZnZn-IMP-78 species, while for the captopril and tiopronin complexes, the dominant peaks correspond to the ternary complexes. It is important to note that relative intensities of the peaks in native mass spectra cannot be unambiguously attributed to relative amounts of species in the samples because it is not certain that all species are equally ionized and vaporized in the mass spectrometer.

Likewise, native MS, UV-vis, and equilibrium dialysis studies suggest that ANT-431 binds to IMP-1 similarly as it binds to VIM-2.[18] Native MS also suggest subtle differences in how the inhibitor interacts with the variants. The dominant peak in the spectra of IMP-1 and IMP-78 with ANT-431 correspond to the ternary complexes, while the spectra for the IMP-6 and IMP-10 complexes show dominant peaks corresponding to the ZnZn- analogs with no inhibitor bound.

The dicarboxylic acid compounds, 3AP-DPA, 1T5PA, and DPA appear to form complexes with IMP-1; however, there is some evidence for metal stripping with these compounds in some experiments. The equilibrium dialysis studies suggest that 3AP-DPA strips more metal from IMP-1 than does 1T5PA or DPA, though the native MS of this sample shows a dominant peak that corresponds to ZnZn-IMP-1 with no 3AP-DPA bound. The native MS of the DPA/IMP-1 sample shows a dominant peak that corresponds to ZnZn-IMP-1 bound to 1 equivalent of DPA. And notably in both cases, there are visible peaks corresponding to Zn-IMP-1 bound to 1 equivalent of 3AP-DPA/DPA. For 1T5PA, the dominant native MS peak corresponds to ZnZn-IMP-1 with no 1T5PA bound. In all the three cases where the dominant peak corresponds to ZnZn-IMP-1 with no inhibitor bound, there were peaks corresponding to the ternary complexes. The UV-vis spectra are difficult to unambiguously interpret, but generally, none of these compounds strip metal to the extent of EDTA. There is also significant broadening of the d-d bands, suggesting an increase in the coordination number of the Co(II) ion(s). The absorbance of the inhibitors alone prevents analysis of intensity changes of the LMCT bands.

IMP-1, NDM-1 and VIM-2 have very low sequence similarities (about 32%), but they globally exhibit a similar αββα sandwich motif albeit with subtle differences in active sites around the dinuclear Zn(II) centers and very distinctive L3 loops.[40, 41] These differences often result in different inhibition properties of the enzymes with the same inhibitor and

different substrate specificities.[40, 41] The studies presented here demonstrate that most of the tested inhibitors bind to IMP-1 similarly as to NDM-1 and VIM-2, but there are subtle differences, as demonstrated by native MS and UV-vis spectroscopy. However, these studies showed that 1T5PA and DPA exhibit different inhibition mechanisms (Table S5) compared to VIM-2 and NDM-1,[9,10] which suggests challenges in using the DPA scaffold for a MBL inhibitor that is effective against all MBLs.

5. Conclusions

In this study, we utilized biochemical techniques combined with spectroscopic techniques to characterize the inhibition mechanism of MBL inhibitors on IMP-1. Importantly, we found that 1T5PA, ANT431, captopril, thiorphan, and tiopronin form ternary complexes. And more surprisingly, 3AP-DPA and DPA showed increased ability for removing the metals comparing to them on NDM-1 but decreased ability to remove metals comparing to them on VIM-2. These inhibitors could be further modified as potentially clinically-viable MBL inhibitors, which provides medicinal therapies for bacterial resistant infections.

Supplementary Material

Refer to Web version on PubMed Central for supplementary material.

Acknowledgements

This work was supported by funding from the National Institutes of Health (GM134454 to MWC; GM128595 to RCP;). Research reported in this publication was supported in part by the National Institute of Allergy and Infectious Diseases of the National Institutes of Health under Awards R01-GM111926 and R01-AI149444. The authors thank Dr. Neil Danielson for assistance in obtaining AAS data.

References:

1. Crowder MW, Spencer J, & Vila AJ (2006). Metallo-β-lactamases: novel weaponry for antibiotic resistance in bacteria. Acc Chem Res, 39(10), 721–728. 10.1021/ar0400241 [PubMed: 17042472]
2. CDC. 2019. Infographic: Antibiotic Resistance the Global threat. https://www.cdc.gov/globalhealth/infographics/antibiotic-resistance/antibiotic_resistance_global_threat.htm. Accessed on December 2019.
3. Naas T, Oueslati S, Bonnin RA, Dabos ML, Zavala A, Dortet L, … & Iorga BI (2017). Beta-lactamase database (BLDB)–structure and function. J Enzym Inhibit Med Chem, 32(1), 917–919. 10.1080/14756366.2017.1344235
4. Papp-Wallace KM, & Bonomo RA (2016). New β-lactamase inhibitors in the clinic. Infect Dis Clin, 30(2), 441–464. doi: 10.1016/j.idc.2016.02.007
5. Bush K, & Bradford PA (2019). Interplay between β-lactamases and new β-lactamase inhibitors. Nature Rev Microbiol, 17(5), 295. 10.1038/s41579-019-0159-8 [PubMed: 30837684]
6. Ju LC, Cheng Z, Fast W, Bonomo RA, & Crowder MW (2018). The continuing challenge of metallo-β-lactamase inhibition: mechanism matters. Trends Pharmacolog Sci, 39(7), 635–647. 10.1016/j.tips.2018.03.007
7. F Mojica M, Bonomo RA, & Fast W (2016). B1-metallo-β-lactamases: where do we stand? Curr Drug Targets, 17(9), 1029–1050. doi: 10.2174/1389450116666151001105622 [PubMed: 26424398]
8. Boyd SE, Livermore DM, Hooper DC, & Hope WW (2020). Metallo-β-lactamases: structure, function, epidemiology, treatment options, and the development pipeline. Antimicro Agents Chemother, 64(10). 10.1128/aac.00397-20

9. Thomas CA, Cheng Z, Yang K, Hellwarth E, Yurkiewicz CJ, Baxter FM, … & Cohen SM (2020). Probing the mechanisms of inhibition for various inhibitors of metallo-β-lactamases VIM-2 and NDM-1. J Inorg Biochem, 210, 111123. 10.1016/j.jinorgbio.2020.111123 [PubMed: 32622213]
10. Fullington S, Cheng Z, Thomas C, Miller C, Yang K, Ju LC, … & Crowder MW (2020). An integrated biophysical approach to discovering mechanisms of NDM-1 inhibition for several thiol-containing drugs. J Biol Inorg Chem, 25, 717–727. 10.1007/s00775-020-01794-z [PubMed: 32500360]
11. Cheng Z, Thomas PW, Ju L, Bergstrom A, Mason K, Clayton D, … & Page RC (2018). Evolution of New Delhi metallo-β-lactamase (NDM) in the clinic: effects of NDM mutations on stability, zinc affinity, and mono-zinc activity. J Biol Chem, 293(32), 12606–12618. 10.1074/jbc.RA118.003835 [PubMed: 29909397]
12. Cheng Z, Shurina BA, Bethel CR, Thomas PW, Marshall SH, Thomas CA, … & Miller CM (2019). A Single Salt Bridge in VIM-20 Increases Protein Stability and Antibiotic Resistance under Low-Zinc Conditions. Mbio, 10(6). 10.1128/MBIO.02412-19
13. Cheng Z, Bethel CR, Thomas PW, Shurina BA, Alao JP, Thomas CA, … & Crowder MW (2021). Carbapenem Use Is Driving the Evolution of Imipenemase 1 Variants. Antimicro Agents Chemother,, 65(4). 10.1128/aac.01714-20
14. Osano E, Arakawa Y, Wacharotayankun R, Ohta M, Horii T, Ito H, … & Kato N (1994). Molecular characterization of an enterobacterial metallo β-lactamase found in a clinical isolate of Serratia marcescens that shows imipenem resistance. Antimicro Agents Chemother, 38(1), 71–78. DOI: 10.1128/AAC.38.1.71
15. Cornaglia G, & Riccio ML (1999). Appearance of IMP-1 metallo-β-lactamase in Europe. The Lancet, 353(9156), 899–900.
16. Griffin DH, Richmond TK, Sanchez C, Moller AJ, Breece RM, Tierney DL, … & Crowder MW (2011). Structural and kinetic studies on metallo-β-lactamase IMP-1. Biochemistry, 50(42), 9125–9134. 10.1021/bi200839h [PubMed: 21928807]
17. Chen AY, Thomas PW, Cheng Z, Xu NY, Tierney DL, Crowder MW, … & Cohen SM (2019). Investigation of Dipicolinic Acid Isosteres for the Inhibition of Metallo-β-Lactamases. ChemMedChem, 14(13), 1271–1282. 10.1002/cmdc.201900172 [PubMed: 31124602]
18. Leiris S, Coelho A, Castandet J, Bayet M, Lozano C, Bougnon J, … & Zalacain M (2018). SAR studies leading to the identification of a novel series of metallo-β-lactamase inhibitors for the treatment of carbapenem-resistant Enterobacteriaceae infections that display efficacy in an animal infection model. ACS Infect Dis, 5(1), 131–140. 10.1021/acsinfecdis.8b00246 [PubMed: 30427656]
19. Brem J, van Berkel SS, Zollman D, Lee SY, Gileadi O, McHugh PJ, … & Schofield CJ (2016). Structural basis of metallo-β-lactamase inhibition by captopril stereoisomers. Antimicro Agents Chemother, 60(1), 142–150. 10.1128/AAC.01335-15
20. Chen AY, Adamek RN, Dick BL, Credille CV, Morrison CN, & Cohen SM (2018). Targeting metalloenzymes for therapeutic intervention. Chem Rev, 119(2), 1323–1455. 10.1021/acs.chemrev.8b00201 [PubMed: 30192523]
21. Siemann S, Clarke AJ, Viswanatha T, & Dmitrienko GI (2003). Thiols as classical and slow-binding inhibitors of IMP-1 and other binuclear metallo-β-lactamases. Biochemistry, 42(6), 1673–1683. 10.1021/bi027072i [PubMed: 12578382]
22. Chen AY, Thomas PW, Stewart AC, Bergstrom A, Cheng Z, Miller C, … & Page RC (2017). Dipicolinic acid derivatives as inhibitors of New Delhi metallo-β-lactamase-1. J Med Chem, 60(17), 7267–7283. 10.1021/acs.jmedchem.7b00407 [PubMed: 28809565]
23. Chen P, Horton LB, Mikulski RL, Deng L, Sundriyal S, Palzkill T, & Song Y (2012). 2-Substituted 4, 5-dihydrothiazole-4-carboxylic acids are novel inhibitors of metallo-β-lactamases. Bioorg Med Chem Lett, 22(19), 6229–6232. 10.1016/j.bmcl.2012.08.012 [PubMed: 22921080]
24. Liu S, Zhang J, Zhou Y, Hu N, Li J, Wang Y, … & Wang J (2019). Pterostilbene restores carbapenem susceptibility in New Delhi metallo-β-lactamase-producing isolates by inhibiting the activity of New Delhi metallo-β-lactamases. Brit J Pharmacol, 176(23), 4548–4557. 10.1111/bph.14818 [PubMed: 31376166]

25. Gasteiger E, Hoogland C, Gattiker A, Wilkins MR, Appel RD, & Bairoch A (2005). Protein identification and analysis tools on the ExPASy server. The Proteomics Protocols Handbook, 571–607. 10.1385/1-59259-890-0:571
26. Queenan AM, Shang W, Flamm R, & Bush K (2010). Hydrolysis and inhibition profiles of β-lactamases from molecular classes A to D with doripenem, imipenem, and meropenem. Antimicro Agents Chemother, 54(1), 565–569. DOI: 10.1128/AAC.01004-09
27. Bergstrom A, Katko A, Adkins Z, Hill J, Cheng Z, Burnett M, Yang H, Aitha M, Mehaffey MR, Brodbelt JS, Tehrani K, Martin NI, Bonomo RA, Page RC, Tierney DL, Fast W, Wright GD, & Crowder MW (2018). Probing the Interaction of Aspergillomarasmine A with Metallo-β-lactamases NDM-1, VIM-2, and IMP-7. ACS Infect Dis, 4(2), 135–145. 10.1021/acsinfecdis.7b00106 [PubMed: 29091730]
28. Leney AC, & Heck AJ (2016). Native mass spectrometry: what is in the name?. J Am Soc Mass Spectrom, 28(1), 5–13. 10.1021/jasms.8b05378 [PubMed: 27909974]
29. Chu YW, Afzal-Shah M, Houang ET, Palepou MFI, Lyon DJ, Woodford N, & Livermore DM (2001). IMP-4, a novel metallo-β-lactamase from nosocomial Acinetobacter spp. collected in Hong Kong between 1994 and 1998. Antimicro Agents Chemother, 45(3), 710–714. DOI: 10.1128/AAC.45.3.710-714.2001
30. Yano H, Kuga A, Okamoto R, Kitasato H, Kobayashi T, & Inoue M (2001). Plasmid-encoded metallo-β-lactamase (IMP-6) conferring resistance to carbapenems, especially meropenem. Antimicro Agents Chemother, 45(5), 1343–1348. DOI: 10.1128/AAC.45.5.1343-1348.2001
31. Iyobe S, Kusadokoro H, Takahashi A, Yomoda S, Okubo T, Nakamura A, & O'Hara K (2002). Detection of a variant metallo-β-lactamase, IMP-10, from two unrelated strains of Pseudomonas aeruginosa and an Alcaligenes xylosoxidans strain. Antimicro Agents Chemother, 46(6), 2014–2016. DOI: 10.1128/AAC.46.6.2014-2016.2002
32. Docquier JD, Riccio ML, Mugnaioli C, Luzzaro F, Endimiani A, Toniolo A, … & Rossolini GM (2003). IMP-12, a new plasmid-encoded metallo-β-lactamase from a Pseudomonas putida clinical isolate. Antimicro Agents Chemother, 47(5), 1522–1528. DOI: 10.1128/AAC.47.5.1522-1528.2003
33. Yang H, Aitha M, Marts AR, Hetrick A, Bennett B, Crowder MW, & Tierney DL (2014). Spectroscopic and mechanistic studies of heterodimetallic forms of metallo-β-lactamase NDM-1. J Am Chem Soc, 136(20), 7273–7285. 10.1021/ja410376s [PubMed: 24754678]
34. Thomas PW, Zheng M, Wu S, Guo H, Liu D, Xu D, & Fast W (2011). Characterization of purified New Delhi metallo-β-lactamase-1. Biochemistry, 50(46), 10102–10113. 10.1021/bi201449r [PubMed: 22029287]
35. D'Costa VM, King CE, Kalan L, Morar M, Sung WW, Schwarz C, … & Golding GB (2011). Antibiotic resistance is ancient. Nature, 477(7365), 457–461. [PubMed: 21881561]
36. Andersson DI, Balaban NQ, Baquero F, Courvalin P, Glaser P, Gophna U, … & Tønjum T (2020). Antibiotic resistance: turning evolutionary principles into clinical reality. FEMS Microbiol Rev, 44(2), 171–188. 10.1093/femsre/fuaa001 [PubMed: 31981358]
37. Atkinson AB, & Robertson JIS (1979). Captopril in the treatment of clinical hypertension and cardiac failure. Lancet, 314(8147), 836–839. 10.1016/S0140-6736(79)92186-X
38. Raczynska JE, Shabalin IG, Minor W, Wlodawer A, & Jaskolski M (2018). A close look onto structural models and primary ligands of metallo-β-lactamases. Drug Resist Updates, 40, 1–12. 10.1016/j.drup.2018.08.001
39. Siemann S, Brewer D, Clarke AJ, Dmitrienko GI, Lajoie G, & Viswanatha T (2002). IMP-1 metallo-β-lactamase: effect of chelators and assessment of metal requirement by electrospray mass spectrometry. Biochim Biophys Acta, 1571(3), 190–200. 10.1016/S0304-4165(02)00258-1 [PubMed: 12090933]
40. Zhang G, & Hao Q (2011). Crystal structure of NDM-1 reveals a common β-lactam hydrolysis mechanism. FASEB J, 25(8), 2574–2582. 10.1096/fj.11-184036 [PubMed: 21507902]
41. Guo Y, Wang J, Niu G, Shui W, Sun Y, Zhou H, … & Rao Z (2011). A structural view of the antibiotic degradation enzyme NDM-1 from a superbug. Prot Cell, 2(5), 384–394. 10.1007/s13238-011-1055-9

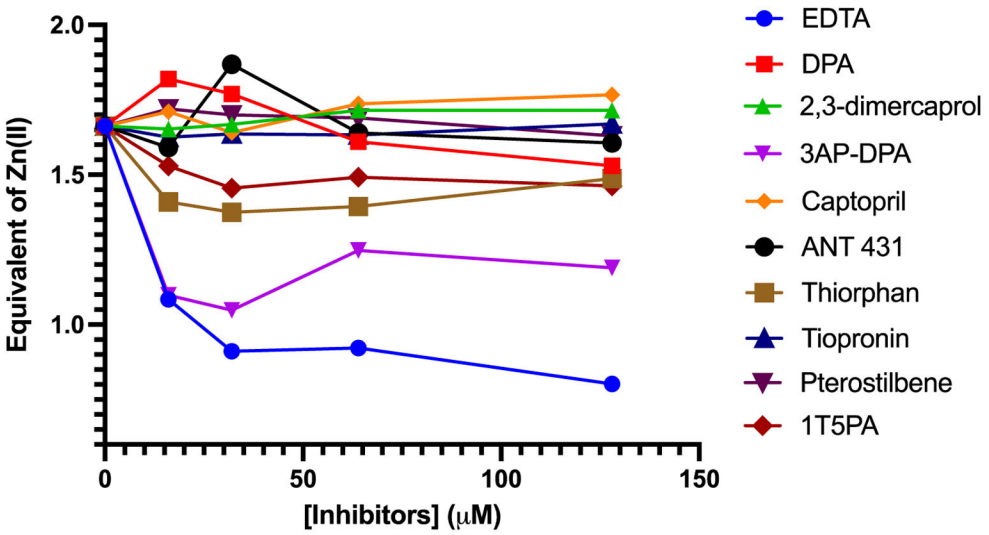

Figure 1: Equilibrium dialyses of IMP-1 with inhibitors.

IMP-1 (8 μM) was incubated with varying concentrations of inhibitor for an hour on ice, and then then the enzyme/inhibitor mixture was dialyzed for 8 hours against 50 mM HEPES, pH 7.5. The metal content of the resulting samples was determined by using atomic absorption spectrometry.[9] The average standard deviation of the Zn content determined by AA is 0.09 μM, as previously reported.[9]

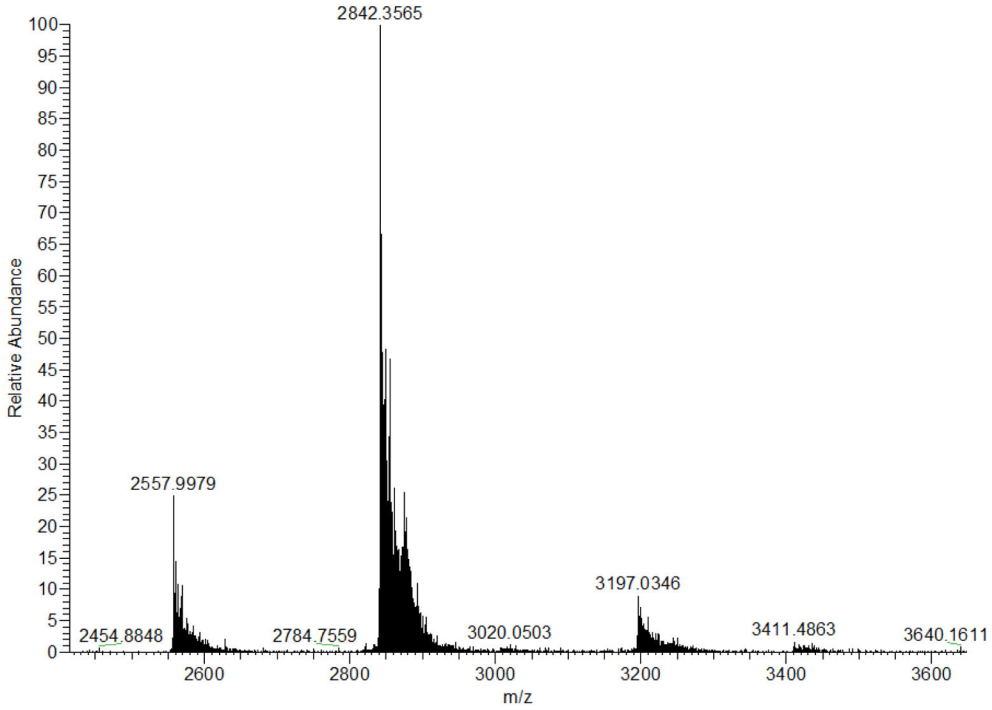

Figure 2: The native MS spectrum for IMP-1 under positive observation mode from 0-4000 *m/z*.
IMP-1 concentration used was 10 μM in 100 mM ammonium acetate, pH 7.5. The dominant peaks are at 2,557.9979 m/z, 2,842.3565 m/z, and 3,197.0346 m/z corresponding to the masses of ZnZn-IMP-1^{10+}, ZnZn-IMP-1^{9+}, and ZnZn-IMP-1^{8+}, respectively.

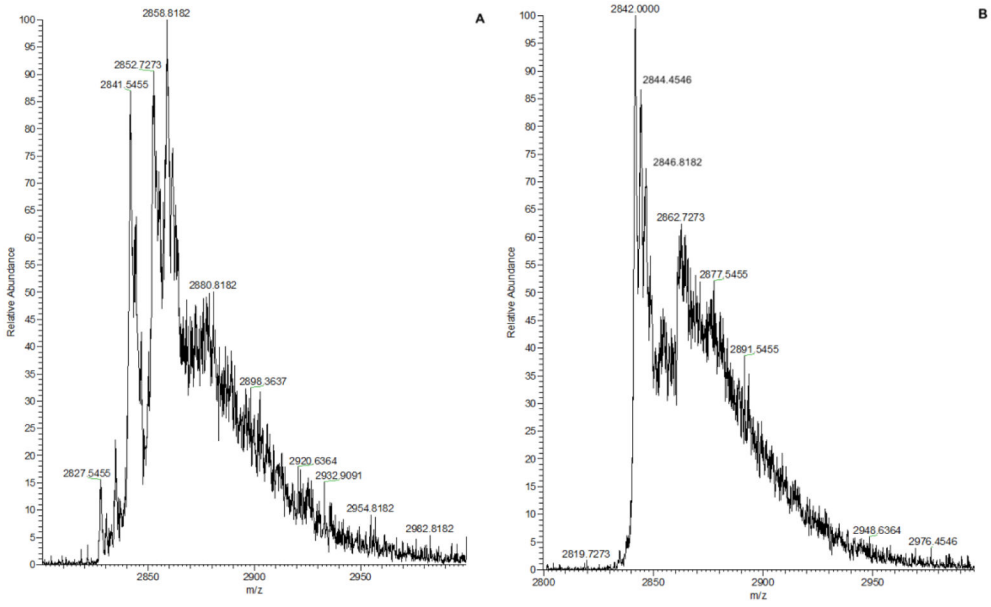

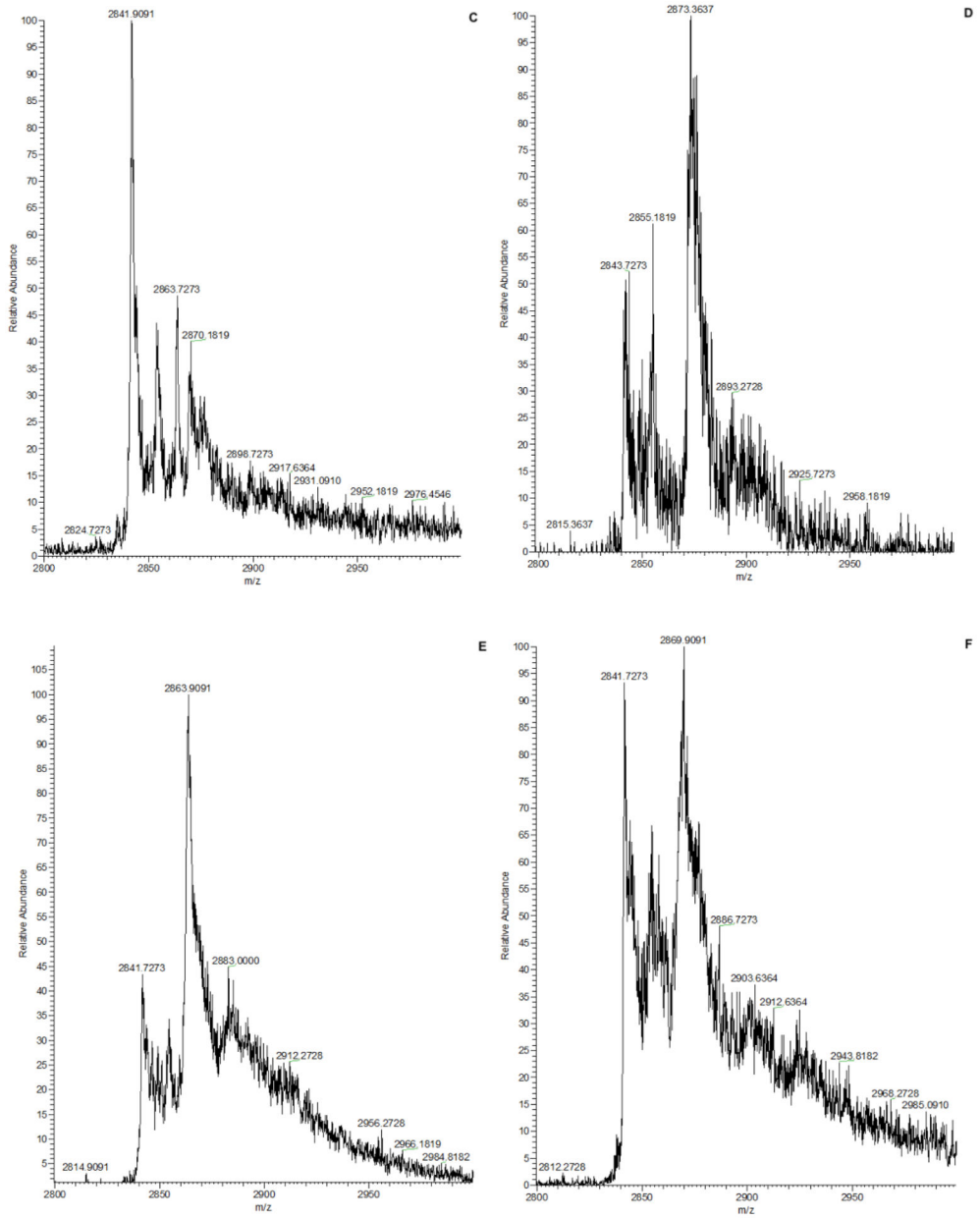

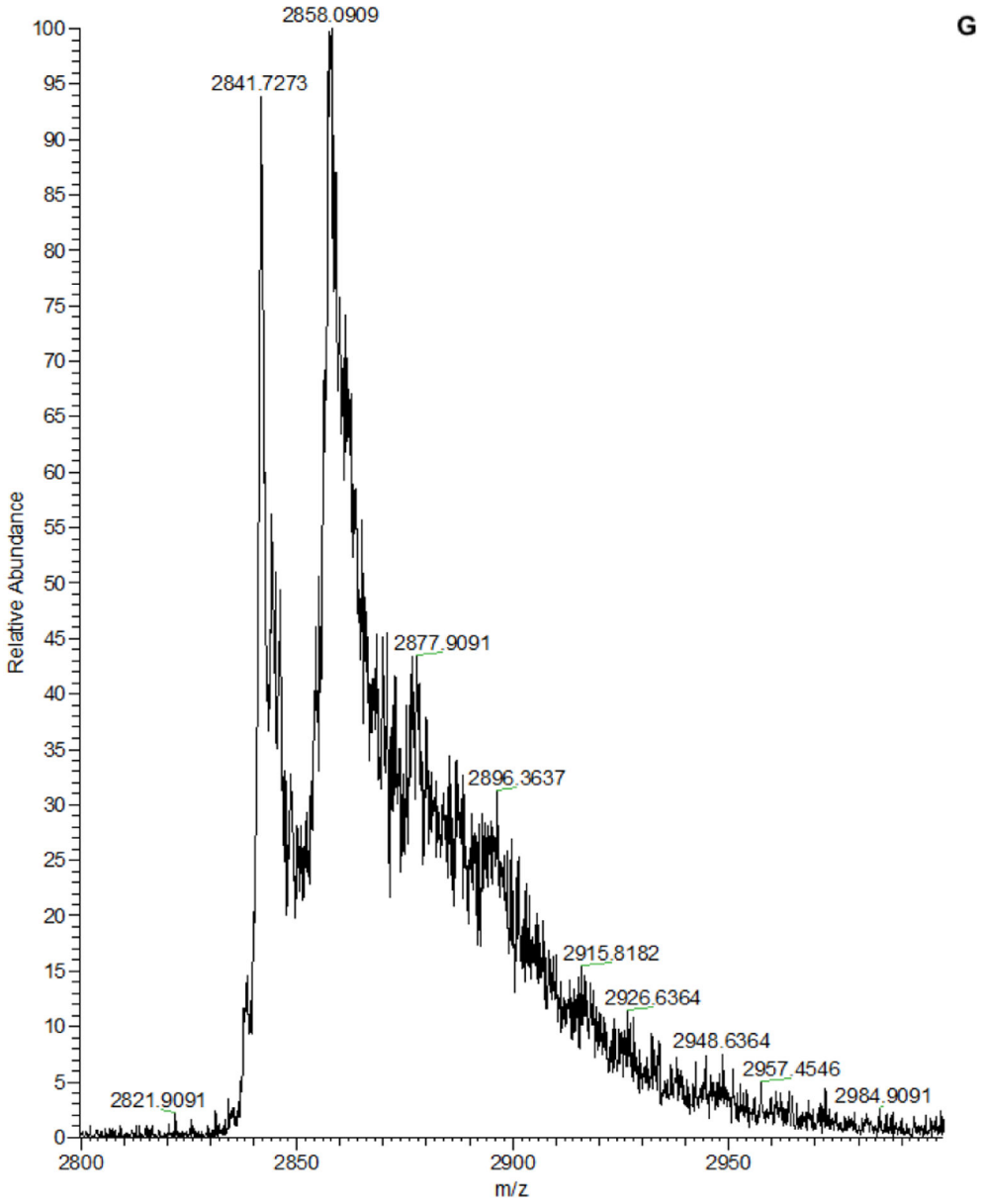

Figure 3: The native MS spectra for IMP-1 bound with inhibitors under positive observation mode from 2800 *m/z* to 3000 *m/z*.

The buffer was 100 mM ammonium acetate, pH 7.5. (A) 10 μM IMP-1 with 5 equivalents of DPA. (B) 10 μM IMP-1 with 5 equivalents of 1T5PA. (C) 10 μM IMP-1 with 5 equivalents of 3AP-DPA. (D) 10 μM IMP-1 with 5 equivalents of ANT431. (E) 10 μM IMP-1 with 5 equivalents of captopril. (F) 10 μM IMP-1 with 5 equivalents of thiorphan. (G) 10 μM IMP-1 with 5 equivalents of tiopronin.

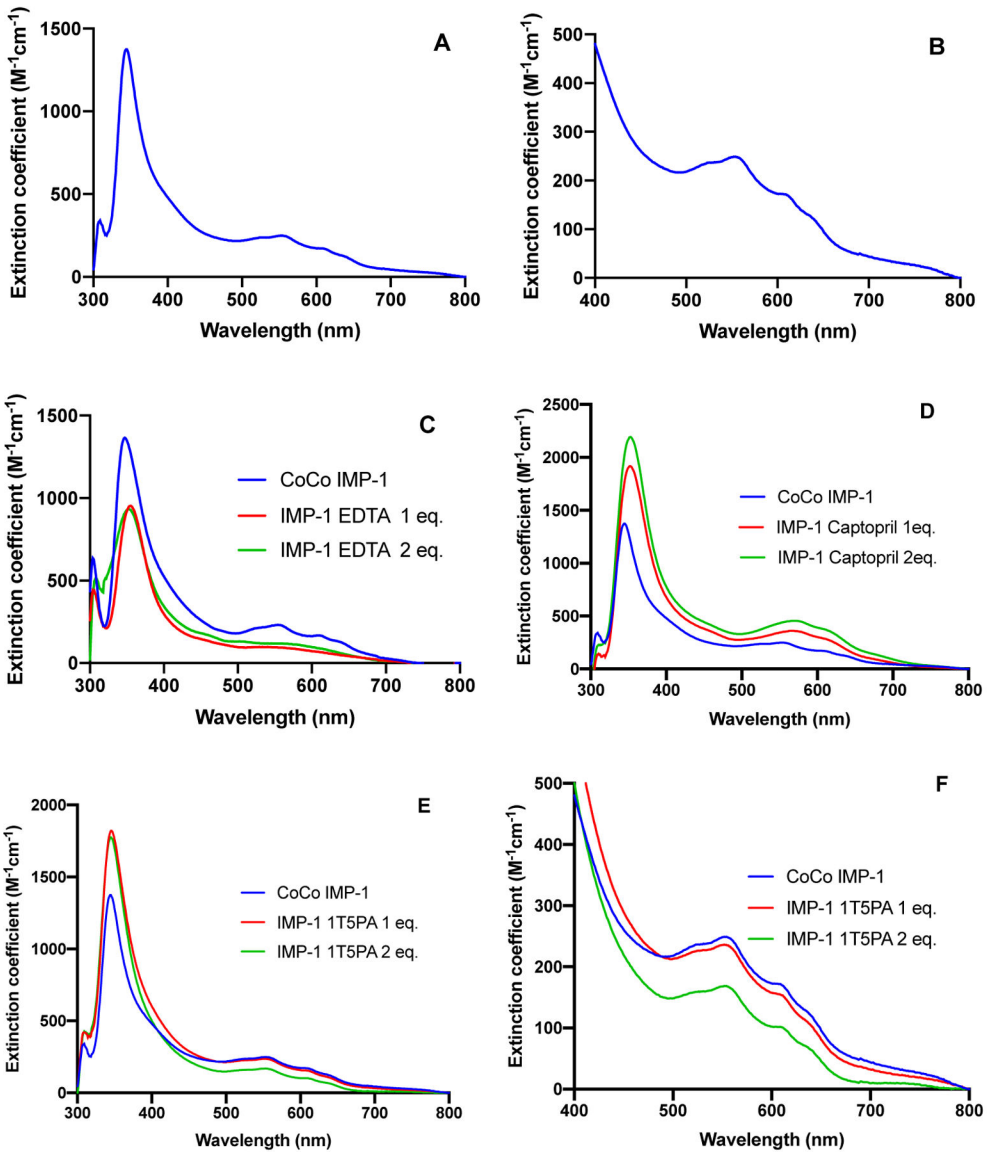

Figure 4: The UV-VIS spectra for CoCo-IMP-1 and CoCo-IMP-1 with EDTA, captopril, and 1T5PA.

The concentration of IMP-1 used in this experiment is 300 μM. (A) The UV-VIS spectrum CoCo-IMP-1. (B) Enlarged view of the spectrum from 400 nm to 800 nm for CoCo-IMP-1. (C) The UV-VIS spectrum after addition of 1 (red) and 2 (green) equivalents of EDTA. (D) The UV-VIS spectrum after addition of 1 (red) and 2 (green) equivalents of Captopril. (E) The UV-VIS spectrum after addition of 1 (red) and 2 (green) equivalents of 1T5PA. (F) The enlarged view of the spectrum from wavelength 400 nm to 800 nm after addition 1 (red) and 2 (green) equivalents of 1T5PA.

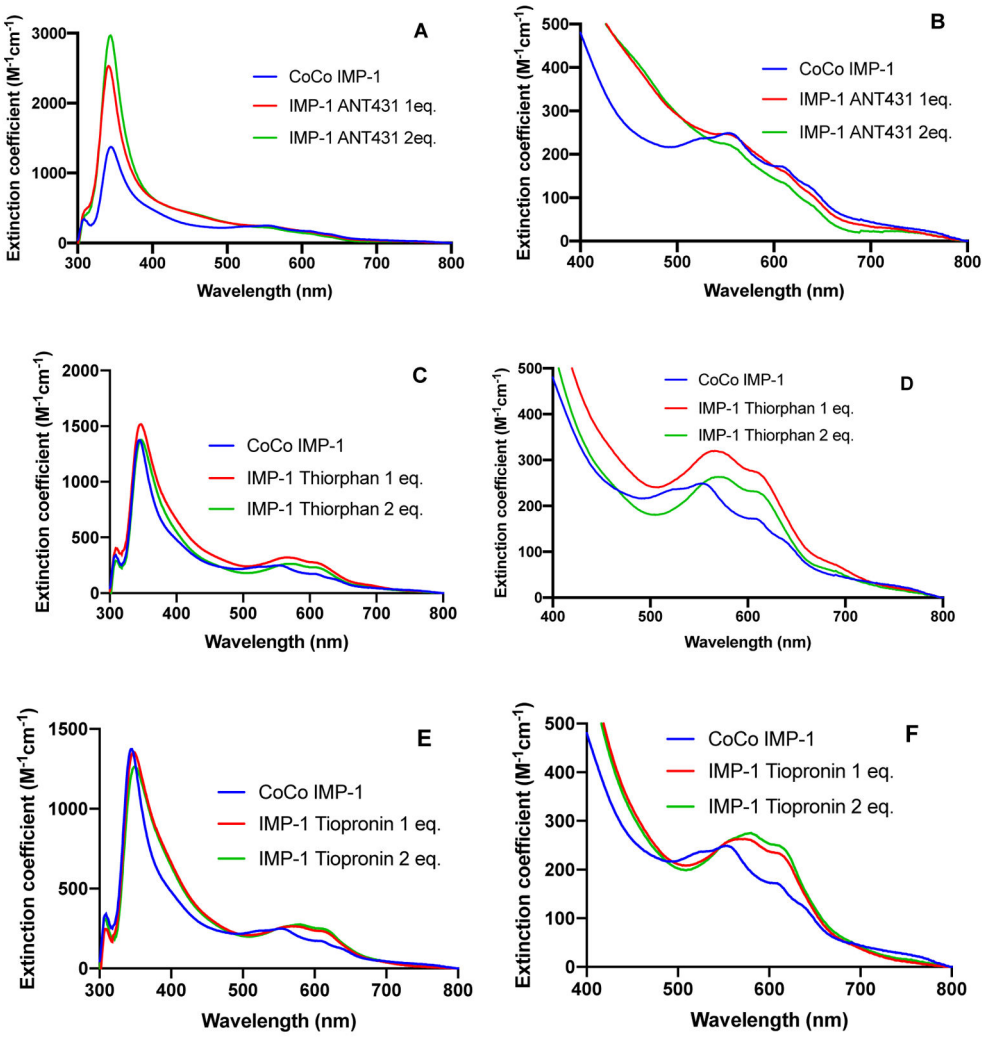

Figure 5: The UV-VIS spectra for CoCo-IMP-1 with ANT431, thiorphan and tiopronin.

The concentration of IMP-1 used in this experiement is 300 μM. (A), (C), (E) The full UV-VIS spectra after additon of 1 (red) and 2 (green) equivalents of ANT431, thiorphan and tiopronin. (B), (D), (F) Enlarged view of the UV-VIS spcetra from 400 nm to 800 nm after addition of 1 (red) and (green) equivalents of ANT 431, thiorphan and tiopronin.

Table 1:

Inhibitors used in this study.

Chemical Structures	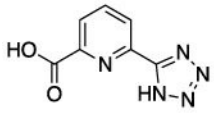	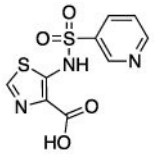	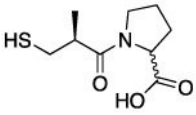	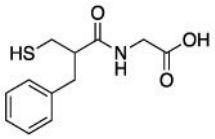	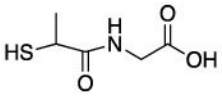
Name Used in this work	1T5PA	ANT431	*D*/*L*-Captopril	Thiorphan	Tiopronin
IC_{50} (μM)[a]	22 ± 1 [17]	54.0 [18]	7.2 ± 1.2 (*D*) 23.3 ± 1.3 (*L*) [19]	N/A	15 [21]
Chemical Structures	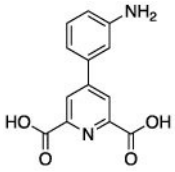	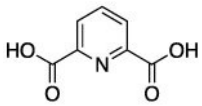	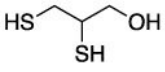	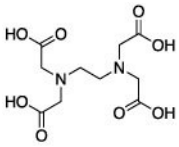	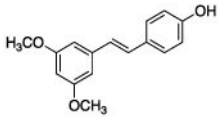
Name Used in this work	3AP-DPA	DPA	2,3-dimercaprol	EDTA	Pterostilbene
IC_{50} (μM)	0.24 ± 0.01 [22]	3.03 ± 0.04 [22]	13 [21]	27.9 [23]	N/A

[a] IC_{50} values are from previous studies on IMP-1.

Table 2:

Theoretical *m/z* and actual *m/z* for ZnZn-IMP-1/6/10/78-inhibitor complexes for the +9 charged ions.

Inhibitors	IMP-1		IMP-6		IMP-10		IMP-78	
	Theoretical *m/z*	Actual *m/z*	Theoretical *m/z*	Actual *m/z*	Theoretical *m/z*	Actual *m/z*	Theoretical *m/z*	Actual *m/z*
ZnZn-IMPs	2841.9833	2,842.3565	2,843.9856	2,844.1819	2,838.6478	2,838.8182	2,847.3222	2,847.2728
1T5PA	2,863.2056	2,862.7273	2,865.2078	2,864.8182	2,859.8700	2,859.8182	2,868.5444	2,868.2728
ANT431	2,873.6824	2,873.3637	2,875.6847	2,877.9091	2,870.3469	2,870.6364	2,879.0213	2,878.6364
Captopril	2,866.127	2,863.9091	2,868.1289	2,867.0000	2,862.7911	2,862.9091	2,871.4656	2,867.4546
Thiorphan	2,870.1300	2,869.9091	2,872.1322	2,870.2728	2,866.7944	2,864.9091	2,875.4689	2,873.3637
Tiopronin	2,860.1167	2,858.0909	2,862.1189	2,859.4546	2,856.7811	2,854.2728	2,865.4556	2,863.0910